Charge Distribution in Bis-Dioxolene Radical Metal Complexes. Synthesis and DFT Characterization of Dinuclear Co(III) and Cr(III) Complexes with a Mixed-Valent, $S = {}^1/_2$ Semiquinone-Catecholate Ligand

Alessandro Bencini,*,† Claude A. Daul,‡ Andrea Dei,*,† Fabio Mariotti,‡ Hyoyoung Lee,§ David A. Shultz,*,§ and Lorenzo Sorace†

Dipartimento di Chimica, Università di Firenze, Firenze, Italy, Departement de Chimie Inorganique et Analitique, Université de Fribourg, Fribourg, Switzerland, and Department of Chemistry, North Carolina State University, Raleigh, North Carolina

Received June 27, 2000

Bis-dioxolene bridged dinuclear metal complexes of general formula $M_2(CTH)_2(diox\text{-}diox)(PF_6)_n$ ($n = 2, 3$; M = Co(III), Cr(III); CTH = tetraazamacrocycle) have been synthesized using the bis-bidentate ligand 5,5′-di-*tert*-butyl-3,3′,4,4′-tetrahydroxybiphenyl. These complexes were characterized by means of ESR, UV−vis, temperature dependent magnetic susceptibility, and cyclic voltammetry. Our results unambiguously suggest that the tripositive dimetal cations can be described as containing a fully delocalized bis-dioxolene trinegative radical ligand (Cat-Sq) bridging two tripositive metal cations. In this frame the sextet electronic ground state characterizes the $Cr_2(CTH)_2(Cat\text{-}SQ)^{3+}$ as a result of the antiferromagnetic coupling of the radical bridging ligand with the two equivalent paramagnetic metal centers. The electronic and geometrical structure and the magnetic properties of Cat-Sq and of its complexes have been studied with density functional theory.

Introduction

Paramagnetic bridging ligands are of considerable interest for the design of materials showing peculiar physical properties. Their utilization for the synthesis of molecular wires, optical switches, and ferro- or ferri-magnetic chains has been proposed from several research groups.[1−8]

Molecules containing linked *o*-dioxolenes may be of considerable interest in this framework because of their redox activity. As shown in Scheme 1, the bis-*o*-quinone (Q-Q) is part of a five-membered redox chain (hereafter Q-Q, Q-Sq, Sq-Sq, Sq-Cat, Cat-Cat) in which all the members are able to act as bis-bidentate ligands.[9,10]

While there is some experimental evidence indicating that the Sq-Sq species is diamagnetic,[10,11] it is still unclear whether the electronic ground state of this molecule is sensitive to the dihedral angle between the dioxolene planes and may therefore change from singlet to triplet. Such a change in ground state spin multiplicity might be expected for torsion angles between dioxolene planes near 90°.[12] The Q-Sq and Sq-Cat members are also paramagnetic, and the Q-Sq and Sq-Cat compounds can be classified as class II or class III mixed-valence systems.[13] In the former case the ligands could serve as molecular switches, in accordance with the existence of two different electronic structures for the two halves of the molecule. On the other hand if the ligands are characterized by delocalized electronic structures, i.e., class III systems, their application for the synthesis of extended molecule-based magnetic materials or molecular wires seems more appropriate. It should be noted that, as far as metal complexes are concerned, much is known about mixed-valence systems formed by metal ions in different oxidation states, but by comparison, little is known about systems containing linked coordinated ligands in different oxidation states.[14,15] The spectroscopic characterization of a mixed-valence compound containing two ruthenium(II) ions bridged by a radical bis(quinonediimine) ligand indicates that the two halves of the ligand are not equivalent, thus suggesting a class II behavior.[16] However, the authors suggest also that a delocalized electronic structure characterizes the bis(semi-

† Università di Firenze.
‡ Université de Fribourg.
§ North Carolina State University.

(1) Kahn, O. In *Modular Chemistry*; Michl, J., Ed.; Kluwer: Dordrecht, 1997.
(2) Gatteschi, D. *Adv. Mater.* **1994**, *6*, 35.
(3) Shultz, D. A.; Boal, A. K.; Driscoll, D. J.; Farmer, G. T.; Holomon, M. G.; Kitchin, J. R.; Miller, D. B.; Tew, G. N. *Mol. Cryst. Liq. Cryst.* **1997**, *305*, 303. Shultz, D. A.; Farmer, G. T. *J. Org. Chem.* **1998**, *63*, 6254. Shultz, D. A.; Boal, A. K.; Farmer, G. T. *J. Org. Chem.* **1998**, *63*, 9462. Shultz, D. A.; Lee, H.; Fico, R. M., Jr. *Tetrahedron* **1999**, *55*, 12079. Shultz, D. A.; Hollomon, M. G. *Chem. Mater.* **2000**, *12*, 580. Caneschi, A.; Dei, A.; Lee, H.; Shultz, D. A.; Sorace, L. *Inorg. Chem.* **2001**, *40*, 408−411. Shultz, D. A.; Bodnar, S. H.; Kampf, J. W. *Chem. Commun.* **2001**, 93−94. Shultz, D. A.; Bodnar, S. H.; Kumar, R. K.; Lee, H.; Kampf, J. W. *Inorg. Chem.* **2001**, *40*, 546−549.
(4) Brandon, E. J.; Rittemberg, D. K.; Arif, A. M.; Miller, J. S. *Inorg. Chem.* **1998**, *37*, 3376.
(5) Woitellier, S.; Launay, J. P.; Joachim, C. *Chem Phys.* **1989**, *131*, 481.
(6) Caneschi, A.; Gatteschi, D.; Renard, J. P.; Rey, P.; Sessoli, R. *J. Am. Chem. Soc.* **1989**, *111*, 785.
(7) Stumpf, H. O.; Ouahabab, L.; Pei, Y.; Bergerat, P.; Kahn, O. *J. Am. Chem. Soc.* **1994**, *116*, 3866.
(8) Nakatani, K.; Carriat, J. Y.; Journaux, Y.; Kahn, O.; Lloret, F.; Renard, J. P.; Pei, Y.; Sletten, J.; Verdaguer, M. *J. Am. Chem. Soc.* **1989**, *111*, 5739.
(9) Joulié, L, F.; Schatz, E.; Ward, M. D.; Weber, F.; Yellowlees, L. J. *J. Chem. Soc., Dalton Trans.* **1994**, 799.
(10) Abakumov, G. A.; Cherkasov, V. K.; Nevodchikov, V. I.; Kuropatov, V. A.; Noll, B. C.; Pierpont, C. G. *Inorg. Chem.* **1998**, *37*, 6117.
(11) Horner, L.; Weber, K.-H. *Chem. Ber.* **1967**, *100*, 2842.
(12) Rajca, A. *Chem. Rev.* **1994**, *94*, 871.
(13) (a) Robin, M. B.; Day, P. *Adv. Inorg. Chem. Radiochem.* **1967**, *10*, 248. (b) Lever, A. B. P. *Inorganic Electronic Spectroscopy*, 2nd ed.; Elsevier: Amsterdam, 1984; p 647.
(14) Penfield, K. W.; Miller, J. R.; Paddon-Row, M. N.; Cotsaris, E.; Oliver, A. M.; Hush, N. S. *J. Am. Chem. Soc.* **1987**, *109*, 5061. Warman, J. M.; De Haas, M. P.; Paddon-Row, M. N.; Cotsaris, E.; Hush, N. S.; Oevering, H.; Verhoeven, J. W *Nature* **1986**, *320*, 615.
(15) Shultz, D. A.; Bodnar, S. H.; Kumar, R. K.; Kampf, J. W. *J. Am. Chem. Soc.* **1999**, *121*, 10664.

10.1021/ic0007052 CCC: $20.00
Published on Web 03/01/2001

Scheme 1

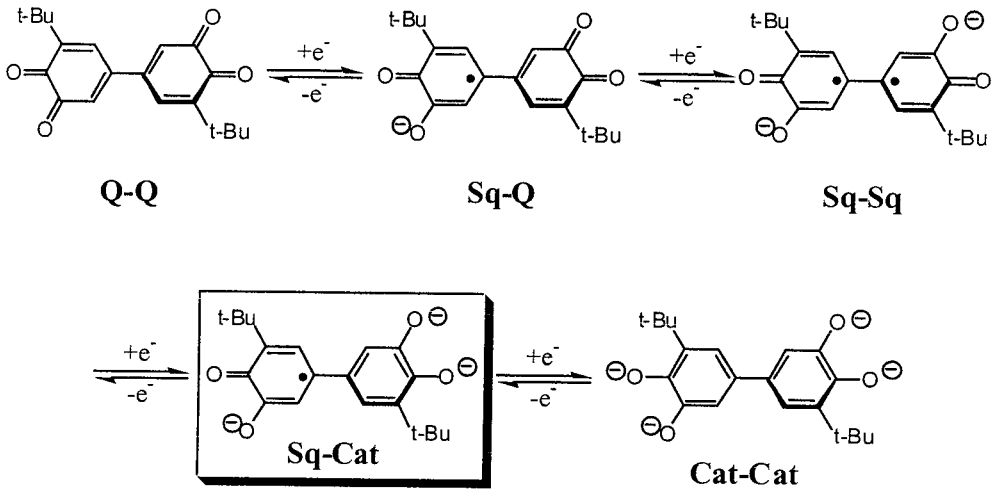

quinonatodiimine) species, the different behavior being due to a different twisting around the central C−C bond.

Since our ligands might behave differently according to different dihedral angles between the dioxolene planes, we felt this subject worthy of an experimental and theoretical investigation. With this in mind, the ligand 5,5′-di-*tert*-butyl-3,3′,4,4′-tetrahydroxybiphenyl was synthesized and used for preparing dinuclear cobalt(III) and chromium(III) metal complexes bridged by the paramagnetic Sq-Cat ligand. The syntheses and the physical properties of the complexes of formulas $(M_2(CTH)_2(Sq\text{-}Cat))(PF_6)_3$ (M = Co, Cr; CTH = *dl*-5,7,7,12,14,14-hexamethyl-1,4,8,11-tetraazacyclotetradecane) are here reported and discussed, together with those of the reduced species containing the $M_2(CTH)_2(Cat\text{-}Cat)^{2+}$ cations.

The classification of mixed-valence systems is not always univocal from experimental data. Some of us have found that quantum-chemical calculations are able to describe the ground state potential energy surfaces of a number of mixed-valent complexes, and therefore they appear to be a valuable tool for the characterization of this class of compounds.[17−19] We have therefore decided to combine quantum-chemical techniques, in the framework of the density functional theory (DFT), to describe the electronic and magnetic structure of the free Sq-Cat ligand and of its complexes. Furthermore, since no crystals suitable for X-ray analysis have been obtained, we calculated their geometries using DFT calculations.

Experimental Section

Synthesis of the Ligand 5,5′-Di-*tert*-butyl-3,3′,4′,4′-tetramethoxybiphenyl (Q-Q). A 100 mL flask containing 5-bromo-1-*tert*-butyl-2,3-dimethoxybenzene[20] (1.31 g, 5.50 mmol), 3-*tert*-butyl-4,5-dimethoxyphenyl-1-boronic acid[20] (1.00 g, 3.66 mmol), Na_2CO_3 (2M, 5.5 mL), ethanol (15 mL), and $Pd(PPh_3)_4$ (212 mg, 0.18 mmol) in toluene (80 mL) was pumped, purged under N_2 five times, and then refluxed for 30 h. After cooling to room temperature, the solvent was removed under reduced pressure. The crude mixture was subjected to SiO_2 column chromatography eluting with 3−5% ether in petroleum ether. The isolated product was recrystallized from ether to give 5,5′-di-*tert*-butyl-3,3′,4,4′-tetramethoxybiphenyl (1.42 g, 99%). ^{1}H NMR ($CDCl_3$) δ (ppm): 7.07 (d, 2H, J = 1.68 Hz), 6.97 (d, 2H, J = 1.68 Hz), 3.93 (s, 12H), 1.44 (s, 18H). ^{13}C NMR ($CDCl_3$) δ (ppm): 153.3, 148.0, 143.4, 136.8, 118.0, 109.9, 60.5, 56.0, 35.3, 30.6. Anal. Calcd for $C_{24}H_{34}O_4$: C, 74.57; H, 8.86. Found: C, 74.40; H, 8.81.

A 250 mL Schlenk flask containing 5,5′-di-*tert*-butyl-3,3′,4,4′-tetramethoxybiphenyl (1.36 g, 3.53 mmol) dissolved in CH_2Cl_2 (120 mL) was cooled to −78 °C, and BBr_3 (2.7 mL, 28.2 mmol) was added slowly via syringe. The reaction mixture was stirred for 1 h at −78 °C and then stirred overnight at room temperature. The reaction was quenched with water to give a white precipitate, which was filtered off to give 5,5′-di-*tert*-butyl-3,3′,4,4′-tetrahydroxybiphenyl (1.16 g, 99%). (Cat-CatH_4) ^{1}H NMR (acetone-d_6) δ (ppm): 7.02 (d, 2H, J = 1.38 Hz), 6.96 (d, 2H, J = 1.38 Hz), 1.47 (s, 18H). Anal. Calcd for $C_{20}H_{26}O_4$: C, 72.70; H, 7.93. Found: C, 72.68; H, 7.92.

Synthesis of the $M_2(CTH)_2(Cat\text{-}Cat)(PF_6)_2\cdot H_2O$ Complexes (M = Co, Cr). These complexes were prepared following the same procedure used for the synthesis of the parent mononuclear M(CTH)-Cat(PF_6) complexes.[21,22] A solution of $M(CTH)Cl_2$ (1 mmol) in methanol (30 mL) was added to a solution of (Cat-CatH_4) (0.45 mmol) in methanol under argon atmosphere. Solid NaOH (2 mmol) was added to the resulting solution. The mixture was gently warmed with stirring for 0.5 h and then cooled to room temperature, and after oxygenation by exposure to the air an aqueous solution of potassium hexafluorophosphate (0.5 g) was dropwise added. A microcrystalline product was obtained. The crude product was purified by column chromatography on silica gel using a 1:2 acetone−dichloromethane mixture as eluent. Anal. Calcd for $C_{52}H_{96}Co_2F_{12}N_8O_5P_2$: C, 47.27; H, 7.32; N, 8.48. Found: C, 47.58; H, 7.49; N, 8.23. Calcd for $C_{52}H_{96}Cr_2F_{12}N_8O_5P_2$: C, 47.78; H, 7.40; N, 8.57. Found: C, 47.63; H, 7.52; N, 8. 31.

Synthesis of the $M_2(CTH)_2(Cat\text{-}SQ)(PF_6)_3\cdot 2H_2O$ Complexes (M = Cr (1), Co (2)). A stoichiometric amount of solid ferrocenium hexafluorophosphate (0.25 mmol) was added to a solution of the above di-hexafluorophosphate derivatives (0.24 mmol) in dichloromethane (20 mL) at room temperature. The resulting solution was stirred for 0.5 h, and then *n*-pentane was added. The resulting microcrystalline precipitate was filtered, washed with *n*-pentane, and then dried in vacuo. Anal. Calcd for $C_{52}H_{98}Co_2F_{18}N_8O_6P_3$: C, 42.14; H, 6.53; N, 7.56. Found: C, 42.34; H, 6.57; N, 7.31. Calcd for $C_{52}H_{98}Cr_2F_{18}N_8O_6P_3$: C, 42.54; H, 6.59; N, 7.63. Found: C, 42.41; H, 6.66; N, 7.51. UV−vis for **1** (E (cm^{-1}), molar absorption in parentheses (M^{-1} cm)): 6300 (sh), 7450 (16400), 9200 (sh), 13500 (sh), 14800 (sh), 15600 (6400), 16400 (6000), 17200 (sh), 21000 (9000), 24100 (17200), 26800 (7800).

(16) Auburn, P. R.; Lever, A. B. P. *Inorg. Chem.* **1990**, *29*, 2553.
(17) Barone, V.; Bencini, A.; Ciofini, I.; Daul, C. A.; Totti, F. *J. Am. Chem. Soc.* **1998**, *120*, 8357.
(18) Bencini, A.; Ciofini, I.; Daul, C. A.; Ferretti, A. *J. Am. Chem. Soc.* **1999**, *121*, 11418.
(19) Ciofini, I.; Daul, C. A.; Bencini, A. In *Recent Advances in Density Functional Methods*; Barone, V., Bencini, A., Fantucci, P., Eds.; World Scientific Publishing Co.: Part III, in press.
(20) Shultz, D. A.; Boal, A. K.; Driscoll, D. J.; Kitchin, J. R.; Tew, G. N. *J. Org. Chem.* **1995**, *60*, 3578.
(21) Benelli, C.; Dei, A.; Gatteschi, D.; Pardi, L. *Inorg. Chim. Acta* **1989**, *163*, 99.
(22) (a) Benelli, C.; Dei, A.; Gatteschi, D.; Güdel, H.; Pardi, L. *Inorg. Chem.* **1989**, *28*, 3089. (b) Resonance Raman spectra on Cr(CTH)-Sq^{2+} complexes (unpublised results from our laboratory) support the assignment of this transition as MLCT.

Physical Measurements. EPR spectra were recorded both for compound **1** and **2** at X-band frequency (9.23 GHz) on a Varian ESR9 spectrometer. The EPR spectrum of compound **2** was recorded at room temperature on a 0.5 mM acetone solution. Polycrystalline powder EPR spectra on compound **1** were recorded at 4.2 K, the spectrometer being equipped with a continuous flow ^{4}He cryostat.

The temperature dependence of magnetic susceptibility between 250 and 4.2 K was measured using a Metronique MS02 SQUID magnetometer with an applied field of 1.0 T. Data were corrected for sample holder contribution and diamagnetism of the sample using standard procedures.[23]

Infrared spectra were recorded on a Perkin-Elmer BX spectrometer. Electronic spectra were recorded in the range 5000−30000 cm^{-1} on a Perkin-Elmer Lambda 9 spectrophotometer. The electrochemical analysis by cyclic voltammetry was carried out by using an electrochemical unit (Amel model 553 potentiostat equipped with Amel 860, 560, and 568 elements) and a classical three-electrode cell. The working electrode was a platinum microsphere, the auxiliary electrode was a platinum disk, and the reference electrode was a calomel electrode in aqueous saturated KCl (SCE). Before each experiment the 1,2-dichloroethane solutions were carefully deaerated with an argon flow. All potentials are reported as referenced versus the ferrocenium/ferrocene couple. Under the experimental conditions used this couple lies at +0.455 V vs SCE.

Computational Details. Calculations were performed with the program packages ADF1999[24] and Gaussian98[25] using density functional theory.[26] Calculations within the local density approximation (LDA) were done using the Xα functional[27] for the exchange part of the functional, and the Vosko, Wilk, and Nusair[28] correlation functional fitting the RPA solution of the uniform electron gas. Generalized gradient approximation (GGA) was applied in the form suggested by Perdew and Wang for the exchange and the correlation.[29]

In order to reduce computer time, the radical ligand Sq-Cat was modeled in all the calculations by substituting the *tert*-butyl groups with methyls, and it will be indicated with the same acronym Sq-Cat in the following. Also the CTH terminal ligands were modeled with ammonia molecules, an approximation which was successfully applied to model other macrocyclic ligands.[17,30] In the geometrical optimizations, the aromatic rings of Sq-Cat have been kept planar, and the ammonia molecules have been considered as rigid bodies with N−H bonds and metal−N−H angles fixed at 1.09 Å and 109.5°, respectively. The quality of the first approximation was checked by fully optimizing the free ligand and the cobalt complex with INDO/1 using the ZINDO method.[31] The computed structures showed a chemically unsignificant deviation of the ring from the planarity (<1° in dihedral angles).

In the calculations performed with ADF1999, the frozen core (FC) approximation for the inner core electrons was used. The orbitals up to 3p for cobalt and 1s for oxygen, carbon, and nitrogen were kept frozen. Valence electrons on each atom were treated with double-ζ basis functions except for the 3d electrons on the metal atoms, which were treated with triple-ζ bases. The valence shells of non-hydrogen atoms were expanded with single-ζ p polarization functions for Co and Cr and with single-ζ d polarization functions for C, O, and N. The exponents of the Slater functions given with the ADF1999.02 distribution were used throughout. The frozen core approximation was relaxed in all the calculations of the isotropic hyperfine coupling constants, which have been computed using the implementation of ADF1999 of the procedure developed by van Lenthe.[32,33] One electron excitation energies were computed using the Slater transition state theory.[27] Intensities of the electronic transitions were estimated by ZINDO/S[31] calculations. INDO/1 and INDO/S calculations were performed with the ZINDO method[31] using the parameters contained in the Hyperchem software package. Electronic transitions were computed with single excitation configuration interaction using 30 occupied × 30 virtual orbitals. Oscillator strengths were calculated in the dipole length approximation. The same method was recently applied to the characterization of the electronic structure of closely related ruthenium complexes.[34]

The potential energy profile of the free ligand as a function of the τ angle (see later in the text) was computed following the linear transit procedure, i.e., as a series of constrained geometrical optimizations at each fixed τ angle in the range 0−180°.

Isotropic hyperfine coupling constants for protons and carbons were also computed with Gaussian98 on the free radical using the EPR-II basis set.[35]

Results and Discussion

Synthesis. The bis(catechol) ligand was prepared as shown below. Previously prepared 5-*tert*-butyl-3,4-dimethoxyphenylboronic acid and 1-bromo-5-*tert*-butyl-3,4-dimethoxybenzene[20] were subjected to Suzuki coupling conditions to give the tetramethyl ether in nearly quantitative yield. The methyl groups were removed by reaction with BBr_3.

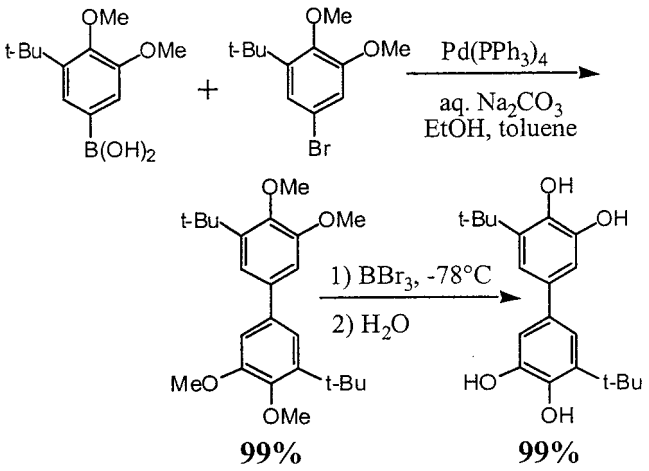

(23) O'Connor, C. J. *Prog. Inorg. Chem.* **1982**, *29*, 203.
(24) *Amsterdam Density Functional (ADF)*; revision 2.3; Scientific Computing and Modelling, Theoretical Chemistry, Vrije Universiteit: Amsterdam, 1997. (a) Baerends, E. J.; Ellis, D. E.; Ros, P. *Chem. Phys.* **1973**, *2*, 42. (b) Boerrigter, P. M.; te Velde, G.; Baerends, E. J. *Int. J. Quantum Chem.* **1988**, *33*, 87. (c) te velde, G.; Baerends, E. J. *J. Comput. Phys.* **1992**, *99*, 84. (d) Fonseca Guerra, C.; Visser, O.; Snijders, J. G.; te Velde, G.; Baerends, E. J. In *Methods and Techniques in Computational Chemistry*; Clementi, E., Corongiu, C., Eds.; STEF: Cagliari, 1995; Chapter 8, p 305.
(25) Frisch, M. J.; Trucks, G. W.; Schlegel, H. B.; Scuseria, G. E.; Robb, M. A.; Cheeseman, J. R.; Zakrzewski, V. G.; Montgomery, J. A., Jr.; Stratmann, R. E.; Burant, J. C.; Dapprich, S.; Millam, J. M.; Daniels, A. D.; Kudin, K. N.; Strain, M. C.; Farkas, O.; Tomasi, J.; Barone, V.; Cossi, M.; Cammi, R.; Mennucci, B.; Pomelli, C.; Adamo, C.; Clifford, S.; Ochterski, J.; Petersson, G. A.; Ayala, P. Y.; Cui, Q.; Morokuma, K.; Malick, D. K.; Rabuck, A. D.; Raghavachari, K.; Foresman, J. B.; Cioslowski, J.; Ortiz, J. V.; Stefanov, B. B.; Liu, G.; Liashenko, A.; Piskorz, P.; Komaromi, I.; Gomperts, R.; Martin, R. L.; Fox, D. J.; Keith, T.; Al-Laham, M. A.; Peng, C. Y.; Nanayakkara, A.; Gonzalez, C.; Challacombe, M.; Gill, P. M. W.; Johnson, B. G.; Chen, W.; Wong, M. W.; Andres, J. L.; Head-Gordon, M.; Replogle, E. S.; Pople, J. A. *Gaussian 98*, revision A.5; Gaussian, Inc.: Pittsburgh, PA, 1998.
(26) Parr, R. G.; Yang, W. *Density Functional Theory of Atoms and Molecules*; Oxford University Press: New York, 1989.
(27) Slater, J. C. *Quantum Theory of Molecules and Solids. Vol. 4: Self-Consistent Field for Molecules and Solids*; McGraw-Hill: New York, 1974.
(28) Vosko, S. H.; Wilk, L.; Nusair, M. *Can. J. Phys.* **1980**, *58*, 1200.
(29) (a) Perdew, J. P.; Wang, Y. *Phys. Rev. B* **1986** *33*, 8800. (b) Perdew, J. P.; Chevary, J. A.; Vosko, S. H.; Jackson, K. A.; Pederson, M. R.; Singh, D. J.; Fiolhais, C. *Phys. Rev. B* **1992**, *46*, 6671.
(30) Gamelin, D. R.; Bominaar, E. L.; Kirk, M. L.; Wieghardt, K.; Solomon, E. I. *J. Am. Chem. Soc.* **1996**, *118*, 8085.
(31) *HyperChem*, release 5.0; Hypercube, Inc.: 1996.
(32) van Lenthe, E.; Wormer, P. E. S.; van der Avoird, A. *J. Chem. Phys.* **1997**, *107*, 2488.
(33) van Lenthe, E.; van der Avoird, A.; Wormer, P. E. S. *J. Chem. Phys.* **1998**, *108*, 4783.
(34) Metcalfe, R. A.; Vasconcellos, L. C. G.; Mirza, H.; Franco, D. W.; Lever, A. B. P. *J. Chem. Soc., Dalton Trans.* **1999**, 2653.

Complexes of formula $M_2(CTH)_2(Cat\text{-}Cat)(PF_6)_2$ (M = Co, Cr) were obtained as microcrystalline powders from the reaction between the $M(CTH)^{2+}$ cations and the Cat-Cat ligand in alkaline methanol under inert atmosphere, followed by oxidation of the metals with air and addition of an aqueous solution of KPF_6. Pure samples of the products were obtained by column chromatography on silica gel using dichloromethane−acetone mixtures as eluents. These complexes can be formulated as chromium(III) and cobalt(III) derivatives on the basis of their magnetic properties and electronic spectra, which are closely related to those of the previously described mononuclear $M(CTH)(DBCat)PF_6$ metal complexes.[21,22] The chromium derivative is characterized by $\chi_M T = 3.7$ ($cm^3\ mol^{-1}\ K$) at room temperature, in agreement with the presence of two noninteracting chromium(III) metal ions, whereas the cobalt complex is obviously diamagnetic. The spectrum of the chromium derivative showed a band at 15300 cm^{-1} ($\epsilon = 180$ cm M^{-1}) (d−d transition) with a shoulder at 26000 cm^{-1}, whereas the cobalt compound shows transitions at 14500 ($\epsilon = 2100$ cm M^{-1}) and 23800 cm^{-1} ($\epsilon = 3150$ cm M^{-1}) (both LMCT in origin) with a shoulder at 19500 cm^{-1} (d−d transition). Therefore it was postulated that these complexes contain dinuclear cations in which the metal ions are bridged by the bis-bidentate tetranegative bis-catecholato ligand anion. The remaining coordination sites are occupied by the macrocyclic ligand that assumes a folded conformation.

Cyclic voltammetry experiments in 1,2-dichloroethane solutions of the chromium complex showed that it undergoes two sequential reversible redox processes at −0.38 and +0.12 V vs the ferrocenium/ferrocene couple (Fc^+/Fc). Both of these processes involve a single electron, as supported by coulometry experiments, and are assigned to redox processes involving the tetraoxolene coordinated ligand. The more negative process is therefore assigned to the Sq-Cat/Cat-Cat couple and the more positive to the Sq-Sq/Sq-Cat one. The observed values are consistent with those reported for a dinuclear ruthenium(II) complex formed by a similar bis(*o*-dioxolene) ligand.[9] The more positive values observed for the chromium derivative can be easily explained by considering the higher oxidation state of the metal ion with respect to that of the ruthenium complex.

The cyclic voltammogram of the cobalt complex is similar: two sequential one-electron, reversible waves at −0.47 and +0.02 V with respect to Fc^+/Fc, which can be assigned as in the chromium complex. A further quasi-reversible redox process is observed at −1.25 V which, in analogy with the electrochemical behavior of mononuclear cobalt dioxolene complexes, can be attributed to the Co(III)/Co(II) couple.[21] It is worth mentioning that the difference between the two ligand-centered redox couples is the same in the two complexes (0.49 and 0.50 V, respectively) and its high value indicates a strong stabilization of the mixed-valence form of the tetroxolene ligand. From these data in fact the comproportionation constant for the equilibrium

$$[M_2(Sq\text{-}Sq)]^{2+} + [M_2(Cat\text{-}Cat)]^{2+} \rightleftharpoons 2[M_2(Sq\text{-}Cat)]^{3+}$$

is ca. 10^6. It is therefore possible to isolate the mixed-valence species without significant presence of the other species. Following this consideration, solid complexes of formula $M_2(CTH)_2(Sq\text{-}Cat)(PF_6)_3$ (M = Co, Cr) were prepared from the above-described bis-catecholato complexes using ferrocenium hexafluorophosphate as oxidizing reagent in dichloromethane and then precipitated as microcrystalline powders by addition of pentane.

Characterization of the Complexes $M_2(CTH)_2(Sq\text{-}Cat)(PF_6)_3$ (M = Co, Cr). The electronic spectrum of the cobalt derivative is shown in Figure 1. It is rather similar to that of the chromium complex, thus indicating that the internal Sq-Cat ligand transitions involving the internal π and π^* levels strongly contribute to the spectra. However, the assignment of charge transfer transition bands is not straightforward. In terms of the usual mixed-valence approach, the pattern of bands appearing in the infrared region of the spectrum could be tentatively assigned to an intramolecular ligand-to-ligand charge transfer in agreement with the assignment made by Lever et al. for a similar transition occurring in the spectrum of a dinuclear ruthenium(II) complex formed by a mixed-valence form of the bis(quinonediimine) ligand.[16] Following these authors, the existence of this transition shifting toward lower energies on increasing the donor power of the solvents (the absorption maximum shifts from 7200 cm^{-1} in dicloroethane to 6950 cm^{-1} in dimethyl sulfoxide) could suggest a class II character to the present metal bridging Sq-Cat ligand. In order to understand the spectral properties a DFT investigation has been carried out, as it will be discussed below.

The electronic spectrum of the chromium derivative shows, in addition to the internal ligand transitions, a band at 20000 cm^{-1} which can be reasonably assigned to a MLCT transition, in analogy with the assignment made for mononuclear Cr(CTH)-Sq^{2+} chromophores.[22,36] The typical sharp transition around 14500 cm^{-1} characterizing all the reported mononuclear chromium(III)−semiquinonato derivatives is not observed, because of its overlapping with the internal ligand transitions.

The EPR spectra of the two $M_2(CTH)_2(Sq\text{-}Cat)(PF_6)_3$ (M = Cr, Co) complexes are shown in Figure 2. The 4.2 K polycrystalline powder spectrum of the chromium derivative (Figure 2a) shows three transitions at 850, 1450, and 1550 G, the last one being a shoulder of the second. These spectral features compare well with that reported in the literature for an $S = {}^5/_2$ spin system split by a large zero field splitting ($|D| > 1$ cm^{-1}) and almost complete rhombicity ($E/D \sim 0.3$).[37] The ESR solution spectrum of the cobalt complex (Figure 2b) shows 17 lines almost equivalently spaced. We attributed this spectral appearance to the hyperfine coupling of the completely delocalized unpaired electron of $SqCat^{3-}$ with two equivalent ^{59}Co ($I_{Co} = {}^7/_2$) nuclei and with two equivalent ^1H nuclei ($I = {}^1/_2$). The expected 45 lines, $(2n_H I_H + 1)(2n_{Co} I_{Co} + 1)$, collapse to 17 due to a line width which is comparable with the hyperfine coupling constant of the electronic spin with the two equivalent protons. The simulation of the spectrum was performed using WIN-EPR SimFonia,[38] a program based on a second-order perturbative solution of the spin Hamiltonian. The simulated spectrum, plotted in Figure 2b (top), was computed with a hyperfine coupling constant for ^{59}Co, $a_{Co} = 4.20$ G, and for ^1H, $a_H = 2.60$ G, using a Gaussian line shape with line width of 2.70 G and $g_{iso} = 2.0$.

The temperature dependence of the magnetic susceptibility of the chromium complex is shown in Figure 3. The solid line represents the fitting of the magnetic data using the three center exchange spin Hamiltonian,

$$H_S = J(\mathbf{S}_1 \cdot \mathbf{S}_2 + \mathbf{S}_2 \cdot \mathbf{S}_3) + J' \mathbf{S}_1 \cdot \mathbf{S}_3 \qquad (1)$$

where $\mathbf{S}_1$ and $\mathbf{S}_3$ are the spin operators of the Cr(III) centers, S_1

(35) Barone, V. In *Recent Advances in Density Functional Methods*; Chong, D. P., Ed.; World Scientific: Singapore, 1995; Part I.
(36) Wheeler, D. E.; McCusker, J. K. *Inorg. Chem.* **1998**, *37*, 2296.
(37) Mabbs, F. E.; Collison, D. *Electron Paramagnetic Resonance of Transition Metal Complexes*; Elsevier: Amsterdam, 1992.
(38) *WIN-EPR SimFonia*, version 1.25; Bruker Analytische Messtechnik GmbH.

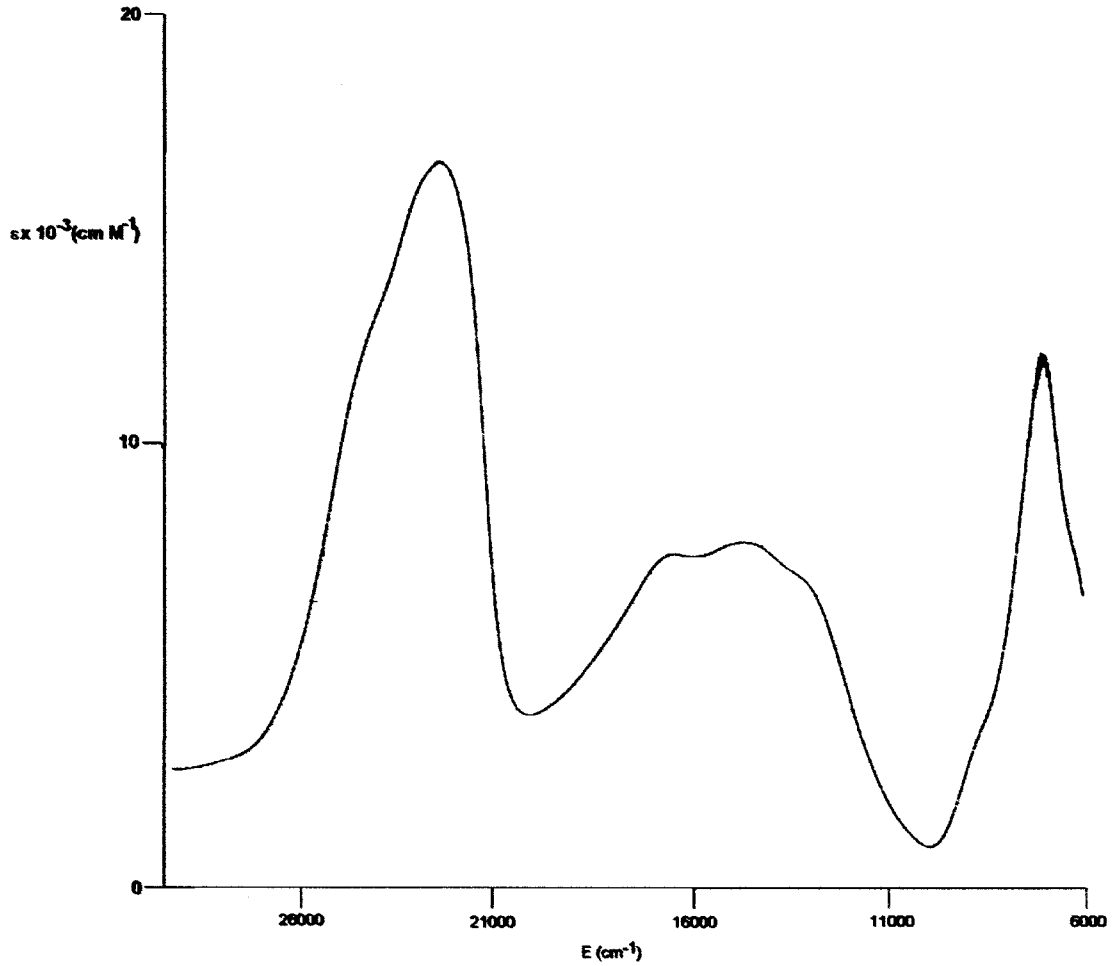

Figure 1. Electronic spectrum of $Co_2(CTH)_2(Sq\text{-}Cat)(PF_6)_3$ in solution of 1,2-dichloroethane.

$= S_3 = {}^3/_2$, and $\mathbf{S}_2$ is the spin of the unpaired electron of the radical ligand. The data were fit by minimizing the sum of the squares of the deviation of the computed χT values from the experimental values, $\sum(\chi_o - \chi_c)^2 T$, using a Simplex minimization procedure. The parameters used in the fit, besides J and J' of eq 1, were the effective isotropic g value and J_{int}, i.e., the effective intramolecular exchange coupling parameter, which accounts for the observed decrease of χT at low temperature. These effects were taken into account in the Weiss molecular field approximation using the equation[23]

$$\chi_c = \frac{\chi}{1 - (J_{int}/Ng^2\mu_B^2)\chi} \qquad (2)$$

Here χ is the molar susceptibility computed in the absence of the interaction and $J_{int} = zj$ is the effective exchange interaction, z being the number of nearest neighbors coupled by the j coupling constant.

The best fit values of the parameters are $g = 1.97(3)$, $J = 743(3)$ cm^{-1}, $J'/J = 0.12(2)$, $J_{int} = -0.14(6)$ cm^{-1} with a residual sum, $s = \sum(\chi_o - \chi_c)^2 T/(n-4) = 0.27 \times 10^{-3}$, n being the number of data. It should, however, be stressed that due to the rather large correlation between the parameters, a situation commonly met in magnetochemistry and not always mentioned in the literature, the range of values for which the fit is satisfactory is quite large. As a matter of fact, equivalent fits can be obtained with values of J and J'/J in a range broader than that indicated by their standard deviations, namely, 500 cm^{-1} $< J <$ 800 cm^{-1} and $0.126 < J'/J < 0.096$.

It can be, however, concluded that the two equivalent Cr(III) paramagnetic centers are antiferromagnetically coupled to the bridging radical ligand, in a way similar to that previously reported for the $Cr_2(CTH)_2(DHBQ)Y_3$ complexes.[39] The ground state of the system is a sextet with the nearest excited states, a quartet and a doublet respectively, lying at 100 ± 11 cm^{-1} and 275 ± 15 cm^{-1} higher in energy.

Electronic and Geometrical Structure of the Ligand Radical Sq-Cat. The geometry of the model radical Sq-Cat^{3-}, optimized at the GGA level of approximation, is reported in Figure 4, where also the relevant bond distances and angles are indicated. The two aromatic rings are not coplanar, their optimized dihedral angle, τ, being 9°. The total energy of Sq-Cat significantly depends on the τ angle, as it is apparent from Figure 5 (see Computational Details). Two regions of minimum energy are computed for $0° \le \tau \le 30°$ and $140° \le \tau \le 170°$, in these ranges the total energies varying by less than 0.6 kcal mol^{-1}. Two independent geometry optimizations with starting values of the τ angle comprised in these two ranges gave two nearly degenerate minima $\tau = 9°$ and 167°, respectively, with an interconversion energy barrier of 7.8 kcal/mol. These structures were used to compute the electronic and spectroscopic properties of the ligand. The energy barrier between the two minima should be high enough to prevent a fluctional behavior of the radical in solution. Both the electronic structure and properties such as hyperfine coupling constants and spin densities are very close when computed for $\tau = 9°$

(39) Dei, A.; Gatteschi, D.; Pardi, L.; Russo V. *Inorg. Chem.* **1991**, *30*, 2589.

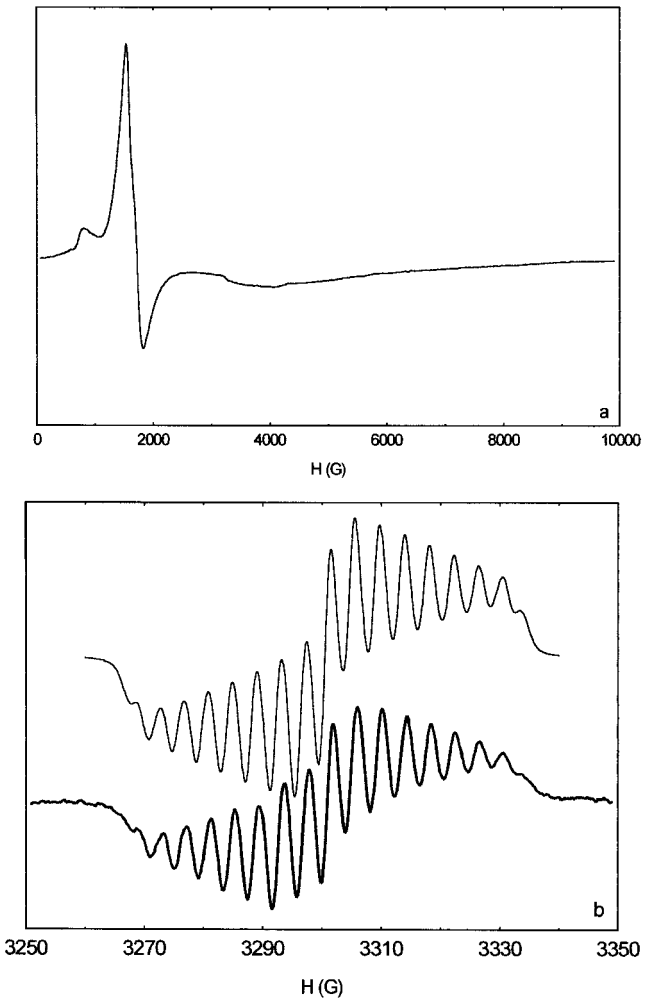

Figure 2. EPR spectra of $M_2(CTH)_2(Sq\text{-}Cat)(PF_6)_3$ (M = Cr, Co): (a) the 4.2 polycrystalline powder spectrum of the Cr derivative; (b) (bottom) the fluid 1,2-dichloroethane solution spectrum of the Co(III) derivative and (top) simulated spectrum as described in the text.

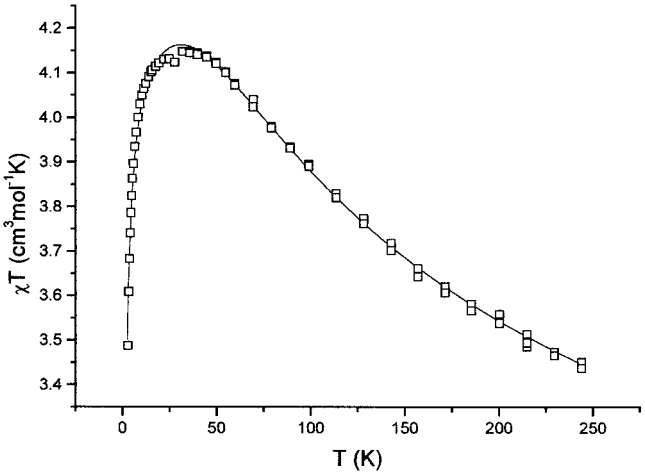

Figure 3. Temperature dependence of the magnetic susceptibility of $Cr_2(CTH)_2(Sq\text{-}Cat)(PF_6)_3$. Solid line represents the fitting of the magnetic data as described in the text.

and 167°, showing that these properties are not strongly dependent on the actual values of τ and therefore this analysis can quite closely represent the real electronic structure of the system. The SOMO is shown graphically in Figure 6, and it is a linear combination of mainly p_z orbitals of carbon and oxygen.

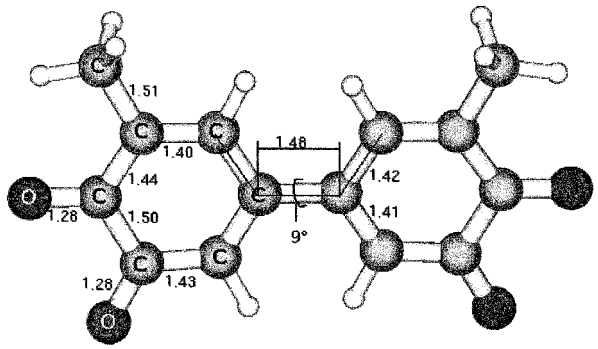

Figure 4. The geometrical structure of the model radical $Sq\text{-}Cat^{3-}$ optimized at the GGA level of approximation.

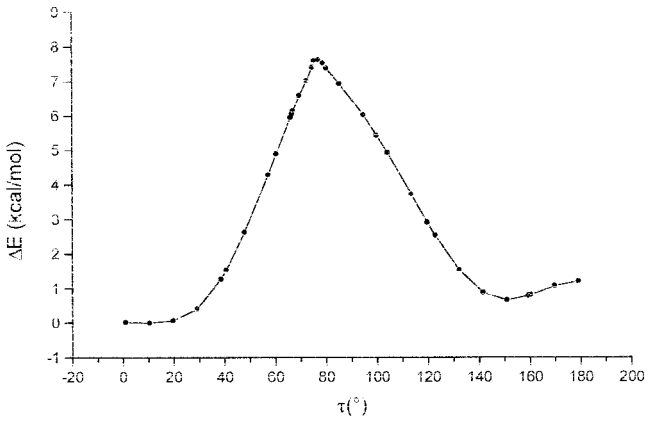

Figure 5. Dependence of the total energy of the model radical $Sq\text{-}Cat^{3-}$ on the dihedral angle τ.

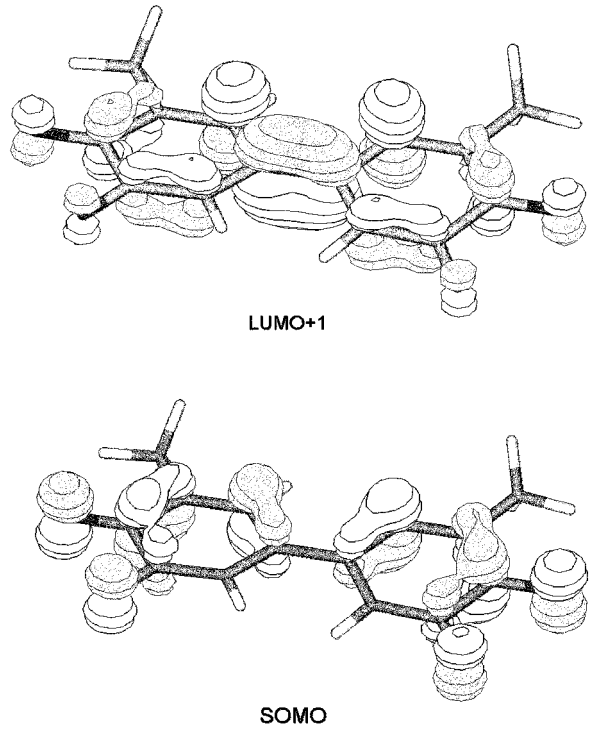

Figure 6. The SOMO orbital of the model radical $Sq\text{-}Cat^{3-}$ and the unoccupied π^* orbital represented as iso surfaces of 0.05 au.

The LUMO region is formed by two accidentally degenerate antibonding orbitals, one mainly localized on the methyl groups, and the other having π^* character. This last orbital, which is the chemically meaningful LUMO, is represented in Figure 6 and labeled LUMO+1.

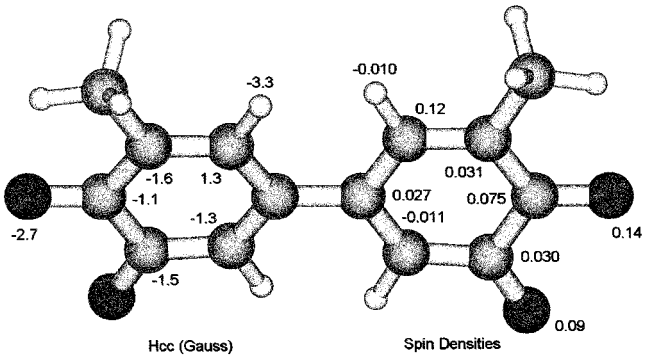

Figure 7. Computed spin densities (right) and ^{1}H and ^{13}C Hfcc (left) for the model radical Sq-Cat^{3-}.

Table 1. Comparison between the Hyperfine Coupling Constants (Gauss) Computed on Sq-Cat^{3-} Using ADF and Gaussian98

nucleus[a]	Gaussian98	ADF
^{13}C	−0.555	−0.721
^{13}C	1.74	1.26
^{13}C	−1.40	−1.31
^{13}C	−0.685	−1.11
^{13}C	−1.63	−1.60
^{13}C	−1.38	−1.51
^{13}C	−0.766	−0.739
^{17}O	−1.81	−2.74
^{17}O	−1.01	−0.047
^{1}H	−0.065	−0.12
^{1}H	0.964	0.810
^{1}H	1.05	0.860
^{1}H	−2.85	−3.32
^{1}H	0.038	0.020

[a] Only the nonequivalent atoms are reported. See Figure 7 for the position of the atoms in the molecule.

The computed Mulliken spin populations are shown in Figure 7. In the same figure also the computed ^{1}H and ^{13}C hyperfine coupling constants (Hfcc) are indicated. These values were computed using nonrelativistic unrestricted calculations. As usually found in catecholato radicals,[40,41] the largest ^{1}H hyperfine coupling constant is computed on the proton ortho to the methyl group. Hyperfine coupling constants were also computed using Gaussian98, for comparison. These figures agree in sign with those computed with ADF and have quite close absolute values. The two sets of coupling constants are compared together in Table 1. The two methods gave comparable results except for one of the ^{17}O for which ADF computes a much smaller HCC (−0.047 vs −1.01 G). We have not at the present any explanation for these figures, and it is also impossible to collect experimental data since the free radical cannot be isolated as such. Further calculations are in progress to clarify this point. A significant part of the spin density is localized onto the oxygen atoms, which are quite different one from the other. Spin polarization effects are evident due to the negative densities computed on some carbon and hydrogen atoms, but, since these values are rather small, spin polarization should not have much relevance in the spin delocalization mechanism.

Electronic and Geometrical Structure of the [Co(NH$_3$)$_4$(Sq-Cat)Co(NH$_3$)$_4$]$^{3+}$ Complex. The geometry of the model complex [Co(NH$_3$)$_4$(Sq-Cat)Co(NH$_3$)$_4$]$^{3+}$ optimized at the GGA level of approximation is shown in Figure 8, where relevant geometrical parameters are also indicated. The two dioxolene rings are significantly non-coplanar, their dihedral angle τ being 47°. The average value of the Co−O bond distance (1.88 Å) is intermediate between the values observed in Co(III)−semiquinonato and Co(III)−catecholato complexes,[42−44] 1.90 and 1.87 Å, respectively, in agreement with the delocalized nature of the unpaired electron. Also the average C−O and the C−C distances (1.34 and 1.42 Å) are close to the average of the values observed in semiquinonato and catecholato complexes, i.e., 1.90 and 1.87 Å for C−O and 1.45 and 1.40 Å for C−C, respectively.[42] The cobalt ion is in a cis-distorted octahedral coordination with a N_2O_2 basal plane. The unpaired electron is delocalized in the SOMO orbital shown in Figure 9. This is close to the SOMO of the free ligand with a small antibonding contribution from out-of-plane π-3d orbitals of the metals. This metallic contribution to the SOMO was evidenced in the ESR spectrum of the complex in the fluid solution.

It should be stressed that the ring linking C−C bond is significantly shorter (1.46 Å) than expected for a single bond. This result should be discussed in light of what was observed by Pierpont et al. for a SQ-SQ derivative.[10]

The electronic spectrum of [Co(NH$_3$)$_4$(Sq-Cat)Co(NH$_3$)$_4$]$^{3+}$ was computed as one-electron excitation from inner doubly occupied orbitals to the SOMO and from the SOMO to the low-lying virtual orbitals using the Slater transition state procedure.[27] The computed transition energies are reported in Table 2 and compared to the experimental spectrum of Co$_2$(CTH)$_2$(Sq-Cat)-(PF$_6$)$_3$ measured in solution. The computed transition energies compare nicely with the experimental data and allowed us to assign the bands at lower energies to intraligand $\pi-\pi^*$ transitions, in agreement with previous observation.[16] The central series of bands (10000−18000 cm^{-1}) is assigned to transitions involving molecular orbitals with a large 3d-Co contribution. The highest energy bands (20000−25000 cm^{-1}) comprise both $\pi-\pi^*$ transitions and metal-to-ligand charge transfer transition, and a more precise assignment is not possible. Due to the difficulty of obtaining transition intensities for this open-shell system, we computed the electronic spectrum also using the ZINDO/S parametrization at the restricted open-shell Hartree−Fock level.[31] The results of the calculation are summarized in Table 3. Strong intensities are computed in the low- and high-energy part of the spectrum in agreement with the suggested assignment.

Electron paramagnetic resonance parameters can be computed within the zero order regular approximation[45] (ZORA) for relativistic effects when the ground state is a Kramers doublet. Using this approach both the **g** and the **A** tensors can be computed. The principal g values, which have to be computed using spin-restricted calculations, are $g_{xx} = 2.004$, $g_{yy} = 2.003$, and $g_{zz} = 2.01$, which gives the average value $g_{iso} = 2.006$, in agreement with the small contribution of the metal orbitals to the SOMO. In order to include spin polarization of the inner core s orbitals, all electron spin unrestricted calculations are needed. Calculations were therefore performed unrestricted using both scalar relativistic ZORA and nonrelativistic Hamiltonians. The computed values were $a_{iso}(^{59}\text{Co}) = 2.12$ and 1.89 G, respectively. The computed hyperfine coupling with the ^{1}H

(40) Felix, C. O.; Sealy, R. C. *J. Am. Chem. Soc.* **1982**, *104*, 1555.
(41) Spenget-Larsen, J. *Int. J. Quantum Chem.* **1980**, *18*, 365.
(42) Pierpont, C. G.; Buchanan, R. M. *Coord. Chem. Rev.* **1981**, *38*, 45.
(43) Pierpont, C. G.; Larsen, S. K.; Boone, S. R. *Pure Appl. Chem.* **1988**, *60*, 1331.
(44) Pierpont, C. G.; Lange, C. W. *Prog. Inorg. Chem.* **1994**, *41*, 331.
(45) (a) van Lenthe, E.; Baerends, E. J.; Snijders, J. G. *J. Chem. Phys.* **1993**, *99*, 4597. (b) van Lenthe, E.; Baerends, E. J.; Snijders, J. G. *J. Chem. Phys.* **1994**, *101*, 9783. (c) van Lenthe, E.; Baerends, E. J.; Snijders, J. G. *J. Chem. Phys.* **1996**, *105*, 6505. (d) van Lenthe, E.; van Leeuwen, R.; Baerends, E. J.; Snijders, J. G. *Int. J. Quantum Chem.* **1996**, *57*, 281. (e) van Lenthe, E.; Ehlers, A. E.; Baerends, E. J. *J. Chem. Phys.* **1999**, *110*, 8943.

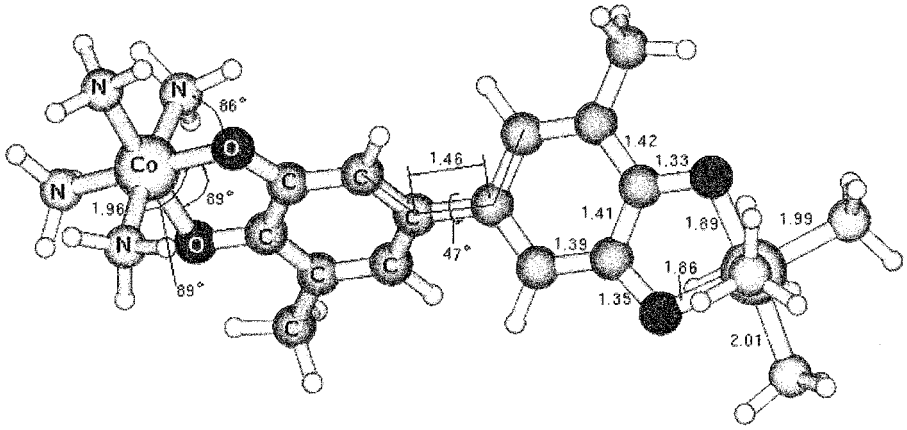

Figure 8. The geometrical structure of the model complex $[Co(NH_3)_4(Sq\text{-}Cat)Co(NH_3)_4]^{3+}$ optimized at the GGA level of approximation.

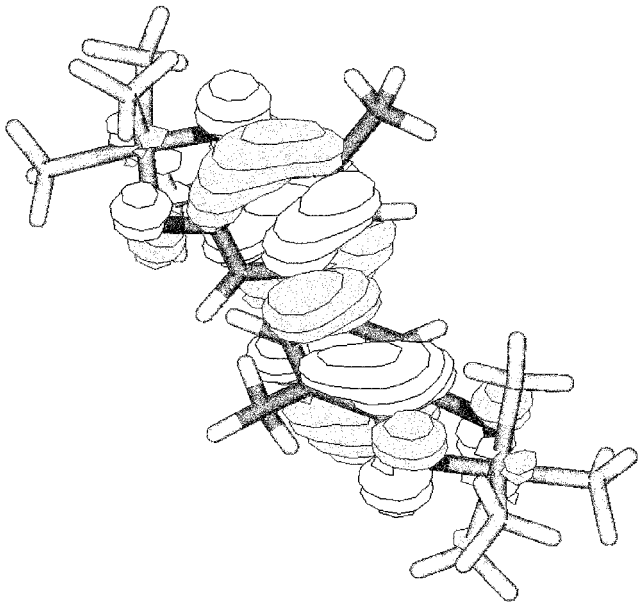

Figure 9. The SOMO orbital of the model complex $[Co(NH_3)_4(Sq\text{-}Cat)Co(NH_3)_4]^{3+}$ represented as iso surfaces of 0.05 au.

nuclei in ortho positions with respect to the methyl groups were, respectively, $a_{iso}(^1H) = 2.12$ and 2.13 G. The calculations agree with the experimental observation of a sizable proton hyperfine coupling, but the hyperfine coupling with the cobalt nucleus is largely underestimated.

Electronic, Geometrical, and Magnetic Structure of the $[Cr(NH_3)_4$ (Sq-Cat)$Cr(NH_3)_4]^{3+}$ Complex. This model complex possesses several spin states arising from the magnetic coupling between the spin of the chromium(III) ions ($S_{Cr} = {}^3/_2$) with the unpaired electron of the Sq-Cat^{3-} radical ligand. The high spin state of the complex has the total spin $S = {}^7/_2$, and it is representable by a single Slater determinant. On this state we have performed the geometry optimization of the model complex, whose structure and relevant geometrical parameters are shown in Figure 10. The molecular structure is close to that of the cobalt(III) complex except for the angle τ, which is now 38°, and the Cr−N bond distances, which are longer, as expected in Cr(III) complexes.

The calculation of the multiplet structure of $[Cr(NH_3)_4$-(Sq-Cat)$Cr(NH_3)_4]^{3+}$ can be performed using the broken symmetry approach (BS) which has been widely applied in the last years.[19,46] This approach is based on a one-to-one correspondence between the SCF energies of appropriate single determinants representing eigenstates of S_z and the diagonal elements

Table 2. Temptative Assignment of the Electronic Spectrum of $Co_2(CTH)_2(Sq\text{-}Cat)(PF_6)_3$ Using DFT Calculations

orbital[a]	energy[b]	assignment[c]	exptl[d]
S−1	4086	L	6100 (s)
S−2	8156	L	7050 (12600)
S−3	9563	L	8400 (s)
LUMO	10243	LM	
L+1	10262	LM	
L+2	11446	LM	12900 (s)
L+3	11536	LM	14200 (8800)
S−4	17766	ML	16200 (8500)
S−5	18487	ML	
S−6	18820	ML	
S−7	20037	ML	
S−8	20011	ML	
S−9	20765	ML	
S−10	24453	L	21900 (16600)
S−11	24652	L	23800 (s)
L+4	24837	ML[e]	
L+5	24813	ML[e]	

[a] Transitions from doubly occupied orbitals to the SOMO are labeled S−*n*, where *n* indicates the *n*th below the SOMO. Transitions from the SOMO to virtual orbitals are labeled L+*n*, where *n* indicates the *n*th level above the LUMO. [b] Transition energies in cm^{-1}. [c] L = transition between states mainly localized on the Sq-Cat^{3-} ligand; LM = transition between an orbital mainly localized on the ligand to an orbital mainly localized on the metal; ML = transition between an orbital mainly localized on the metal to an orbital mainly localized on the ligand. If not specified the ligand is the Sq-Cat^{3-} one. [d] The value of ϵ ($cm\ M^{-1}$) is shown in parentheses; s = shoulder. [e] Metal to NH_3 charge transfer.

Table 3. Electronic Spectrum of $[Co(NH_3)_4(Sq\text{-}Cat)Co(NH_3)_4]^{3+}$ Computed Using ROHF-ZINDO/S Calculation[a]

$[Co(NH_3)_4(Sq\text{-}Cat)Co(NH_3)_4]^{3+}$
6138 (0.28)
11737 (0.02)
22795 (0.02)
23081 (0.04)
23101 (0.10)

[a] Energies (cm^{-1}) of the transitions between 4000 and 27000 cm^{-1}. Oscillator strengths >0.01 are reported in parentheses.

of the spin Hamiltonian (eq 1) in a basis set of products of single center spin functions. The total spin states arising from the magnetic interaction can be labeled using the eigenvalue of the

(46) (a) Noodleman, L.; Norman, J. G., Jr. *J. Chem. Phys.* **1979**, *70*, 4903. (b) Noodleman, L. *J. Chem. Phys.* **1981**, *74*, 5737. (c) Bencini, A. *J. Chim. Phys.* **1989**, *86*, 763. (d) Noodleman, L.; Peng, C. Y.; Case, D. A.; Mouesca, J. M. *Coord. Chem. Rev.* **1995**, *144*, 199. (e) Bencini, A.; Totti, F.; Daul, C. A.; Doclo, K.; Fantucci, P.; Barone, V. *Inorg. Chem.* **1997**, *36*, 5022.

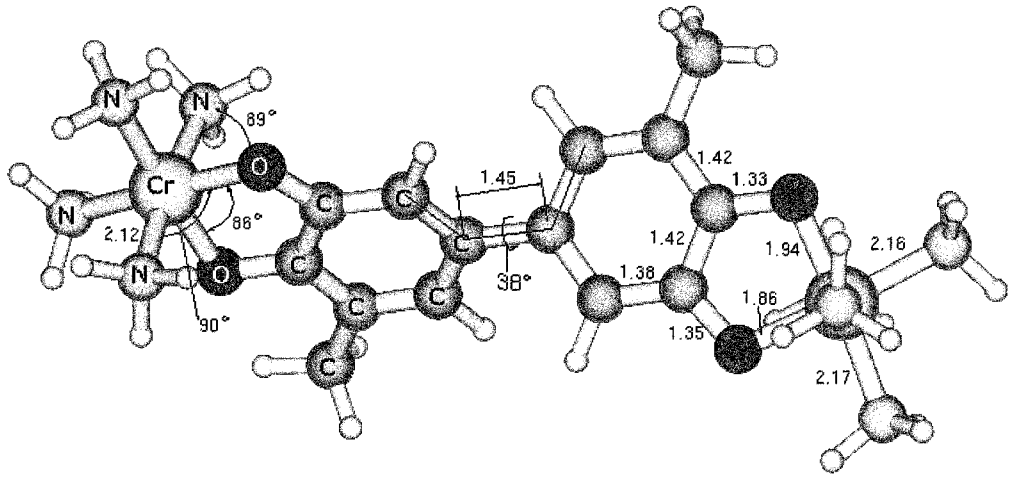

Figure 10. The geometrical structure of the model complex $[Cr(NH_3)_4(Sq\text{-}Cat)Cr(NH_3)_4]^{3+}$ optimized at the GGA level of approximation.

intermediate spin operator $\mathbf{S}_{13}^2 = (\mathbf{S}_1 + \mathbf{S}_3)^2$ and of the total spin $\mathbf{S}^2 = (\mathbf{S}_{13} + \mathbf{S}_2)^2$ and S_z, i.e., with kets $|S_{13}SM_S\rangle$. In the product basis of the three spin function $\{|m_1m_2\rangle m_3\rangle\} \equiv \{|s_1 m_1\rangle|s_2m_2\rangle|s_3m_3\rangle\}$ we can write the spin eigenfunction corresponding to the high spin state $S = {}^7/_2$ and $M_S = {}^7/_2$, namely, $|3\ {}^7/_2\ {}^7/_2\rangle = |{}^3/_2\ {}^1/_2\ {}^3/_2\rangle$, and to the antiparallel spin state, corresponding to $M_S = {}^5/_2$, namely, $|{}^5/_2\rangle = |{}^3/_2\ -{}^1/_2\ {}^3/_2\rangle$. This last wave function is not an eigenfunction of $\mathbf{S}^2$, but only of S_z, and it can be also called the antiferromagnetic, AF, state. These two spin arrangements can be associated with two single Slater determinants called the high spin state and the broken symmetry state, BS_1. Since single determinants cannot, in the general case, represent spin eigenfunction and hence their energies are not the energies of the spin multiplets, their energies are associated in a first approach to the diagonal elements of H_S, or, alternatively, spin projection techniques and decomposition of these energies in terms of pure multiplet energies are applied. A second rather widely used approach assumes that the largest part of the electron correlation, both static and dynamic, is accounted for by the functional of the electron density and associates these energies to the pure state energies obtained from the diagonalization of the spin Hamiltonian (eq 1).[47] With this last approach a better agreement with the experimental data is generally achieved, although it has been recently found that the modeling of the real system can be crucial in judging the agreement between spin Hamiltonian parameters calculated on model complexes and the experimental data.[19] In this paper we will follow both approaches, the relevant equations for for the first and second approach being eqs 2 and 3 and eqs 4 and 5, respectively.

Using the energy of the single determinants, $E(HS)$ and $E(BS_1)$, obtained by independent SCF convergences we can calculate the J value, in the first approach, according to

$$E(HS) - E(BS_1) = 3J \tag{2}$$

The calculation of J' requires the evaluation of the energy of another determinant which can be easily set up by the spin configuration $|{}^3/_2\ {}^1/_2\ -{}^3/_2\rangle$. This is an eigenstate of S_z with eigenvalue ${}^1/_2$ and will be indicated as BS_2. The relevant equation is

$$E(HS) - E(BS_2) = {}^3/_2J + {}^9/_2J' \tag{3}$$

The equations relevant for the calculation of J assuming that the single determinant energies are close to the multiplet energies, i.e., using the second approach, are

$$E(HS) - E(S_{13} = 3, S = {}^5/_2) = {}^7/_2J \tag{4}$$

$$E(HS) - E(S_{13} = 0, S = {}^1/_2) = {}^3/_2J + 6J' \tag{5}$$

Spin Hamiltonian parameters obtained by eqs 2 and 3 and eqs 4 and 5 represent limiting values, the exact values being between these two extrema. The computed values of J for $[Cr(NH_3)_4(Sq\text{-}Cat)Cr(NH_3)_4]^{3+}$ are $J = 590\ cm^{-1}$, $J' = 11.4\ cm^{-1}$ and $J = 506\ cm^{-1}$, $J' = 29.6\ cm^{-1}$, using eqs 2 and 3 and eqs 4 and 5, respectively. With both sets of parameters the ground spin multiplet is $|3\ {}^5/_2\rangle$ with next excited states $|2\ {}^3/_2\rangle$ and $|1\ {}^1/_2\rangle$ at 261 and 534 cm^{-1}, and at 164 and 360 cm^{-1}, respectively. These findings are in nice qualitative agreement with the results of the fitting of the magnetic susceptibility data, which gave the $|3\ {}^5/_2\rangle$ state as the ground state with the $|2\ {}^3/_2\rangle$ and the $|1\ {}^1/_2\rangle$ states at $100 \pm 11\ cm^{-1}$ and $275 \pm 15\ cm^{-1}$, respectively.

Conclusions

The combined use of DFT and spectroscopic data allowed us to achieve a deep understanding of the electronic structure of the $M_2(CTH)_2(Sq\text{-}Cat)(PF_6)_3$ ($n = 3$; M = Co(III), Cr(III); CTH = tetraazamacrocycle) complexes. In particular, our results strongly suggest a fully delocalized electronic structure description for the trinegative radical ligand 5,5′-di-*tert*-butyl-3,3′,4,4′-tetraoxobiphenyl and their homodinuclear metal complexes. This description is independent from the value of the dihedral angle between the phenyl rings, taking into account the existence of a binary symmetry axis within the molecule. Therefore, if the current chemical terminology is used, as we have done in the text, a description of the Sq-cat ligand as a class III mixed valence species seems appropriate. This conclusion, however, cannot in principle hold if the symmetry of the bis-dioxolene molecule is broken by introducing different ring substituents or by coordination to different metal ions.

IC0007052

(47) (a) Ruiz, E.; Alemany, P.; Alvarez, S.; Cano, J. *J. Am. Chem. Soc.* **1997**, *119*, 1297. (b) Ruiz, E.; Cano, J.; Alvarez, S.; Alemany, P. *J. Am. Chem. Soc.* **1998**, *120*, 11122.